JVI Journals.ASM.org

Bilateral Entry and Release of Middle East Respiratory Syndrome Coronavirus Induces Profound Apoptosis of Human Bronchial Epithelial Cells

Xinrong Tao,[a] Terence E. Hill,[a] Chikao Morimoto,[d] Clarence J. Peters,[a,c] Thomas G. Ksiazek,[b] Chien-Te K. Tseng[a,c]

Departments of Microbiology and Immunology[a] and Pathology[b] and Center for Biodefense and Emerging Infectious Disease,[c] University of Texas Medical Branch, Galveston, Texas; Department of Therapy Development and Innovation for Immune Diseases and Cancer, Juntendo University, Tokyo, Japan[d]

The newly emerged Middle East respiratory syndrome coronavirus (MERS-CoV) infects human bronchial epithelial Calu-3 cells. Unlike severe acute respiratory syndrome (SARS)-CoV, which exclusively infects and releases through the apical route, this virus can do so through either side of polarized Calu-3 cells. Infection results in profound apoptosis within 24 h irrespective of its production of titers that are lower than those of SARS-CoV. Together, our results provide new insights into the dissemination and pathogenesis of MERS-CoV and may indicate that the virus differs markedly from SARS-CoV.

Recently, a novel human coronavirus (CoV) causing acute pneumonia with renal failure emerged in the Middle East. Between June 2012 and 22 May 2013, infections caused by this virus, now called Middle East respiratory syndrome (MERS)-CoV (1), resulted in 21 deaths among 43 confirmed cases worldwide (2). Such an alarming mortality rate of close to 50% has reignited public concern about its potential for resulting in a pandemic like that of the 2002-to-2003 outbreak of severe acute respiratory syndrome (SARS) that emerged first in Asia, eventually killing 774 of ~8,000 infected individuals worldwide (3). Built on the platform established over the last decade in dealing with the SARS epidemic, tremendous progress toward unraveling the genome, cellular tropism, and susceptibility to biological intervention has been achieved at an unprecedented speed. Based on genomic and phylogenetic analyses, MERS-CoV belongs to the lineage c beta (β)-CoVs and is more closely related to Asian bat CoVs than to other β-CoVs, including SARS-CoV (lineage b), OC43, and HKU1 (human viruses in lineage a) (4). While SARS-CoV utilizes human angiotensin-converting enzyme 2 (hACE2) as the functional receptor (5–7), MERS-CoV exploits an evolutionarily conserved CD26/dipeptidyl peptidase 4 (DPP4) molecule to enter permissive cells of different mammalian species (8). While MERS-CoV, like SARS-CoV, readily infects differentiated primary human airway epithelial cells (HAEC) and releases infectious progeny virus predominantly through the apical surface, it seems to be more vulnerable than SARS-CoV to prior alpha interferon (IFN-α) treatment (9). While these findings have significant implications for the development of effective strategies against this newly emerged human respiratory viral disease, a better understanding of how this virus interacts with host cells will be crucial for advancing the current knowledge of MERS-CoV pathogenesis. In particular, unveiling the distribution of the entry CD26/DPP4 receptor, on the membrane of HAEC, the main portal of entry of respiratory pathogens, and the subsequent outcome of MERS-CoV infection still await full investigation.

We previously showed that polarized human bronchial epithelial Calu-3 cells are susceptible to ACE2-mediated SARS-CoV infection exclusively through the apical surface accompanied by the release of infectious progeny virus predominantly via the apical surface (10). In this study, we first compared the infectivity characteristics of SARS-CoV and MERS-CoV in Calu-3 cells and three other SARS-CoV-permissive human cell lines, i.e., the naturally ACE-2-expressing colonic epithelial LoVo cells and alveolar epithelial A549 and embryonic kidney 293 cells, both of which stably express ACE-2 following transfection (5, 11). SARS-CoV (Urbani) and MERS-CoV (EMC-2012) were used throughout this study. As shown in Fig. 1A, MERS-CoV replicated to titers of 10^5 to 10^6 at 24 h postinfection (pi) in both Calu-3 and LoVo cells but not in ACE-2-expressing A549 or 293 cells, confirming the ACE-2-independent nature of MERS-CoV infection (12). We also noted that the 24-h infection was in striking contrast to the delayed development of a microscopically visible cytopathic effect (CPE), which usually does not occur until day 5 pi, at the earliest, in SARS-CoV-infected Calu-3 cells (10), and that MERS-CoV infection resulted in extensive detachment of the monolayer within 24 h, an observation consistent with recent reports (13, 14). Further, the formation of such an acute and profound CPE seemed to be specific to infected Calu-3 cells, as it took at least 4 days for infected LoVo cells to show ~10% to 15% CPE (data not shown). We also established the "one-step" growth curves of MERS-CoV versus SARS-CoV in Calu-3 cells by using a multiplicity of infection (MOI) of 3. Despite the fact that MERS-CoV failed to replicate as dynamically as SARS-CoV at both 8 and 32 h pi ($P < 0.01$) (Fig. 1B), it consistently induced readily detectable CPE at 16 h with ~20% monolayer detachment, which rapidly progressed to 70% and 100% at 24 and 32 h pi, respectively (data not shown). As anticipated, we did not observe any CPE in SARS-CoV-infected cultures at day 4 when the experiment was terminated. Since it has been demonstrated that CD26/DPP4 expression on cells of nonlymphoid origin, such as African green monkey COS-7 fibroblasts, confers their susceptibility to MERS-CoV infection (8), we asked whether expression of CD26/DPP4 on lymphoid cells could

Received 27 June 2013 **Accepted** 27 June 2013
Published ahead of print 3 July 2013
Address correspondence to Chien-Te K. Tseng, sktseng@utmb.edu.

doi:10.1128/JVI.01562-13

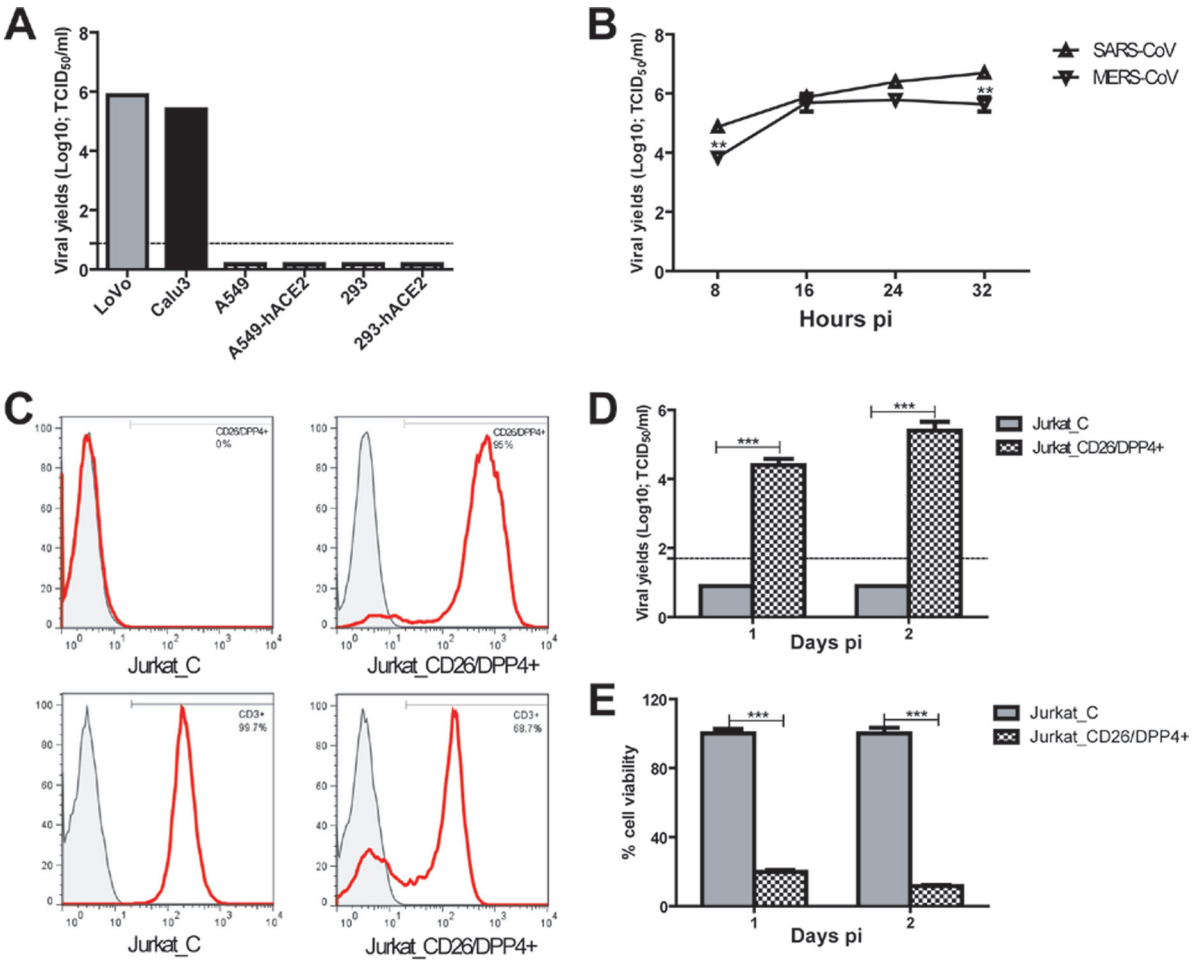

FIG 1 Human bronchial epithelial Calu-3 cells, colonic LoVo epithelial cells, and CD26/DPP4-expressing human Jurkat T cells are permissive for MERS-CoV/EMC-2012 infection. (A) Confluent Calu-3 cells, LoVo cells, alveolar A549 cells, ACE2-expressing A549 cells, embryonic kidney 293 cells, and ACE2-expressing 293 cells, grown in 12-well plates, were infected with MERS-CoV/EMC-2012 at an MOI of 0.1 for 24 h before harvesting of cell-free supernatants for assessing infectious viral titers by the standard Vero E6-based 50% tissue culture infective dose ($TCID_{50}$) assay. (B) The "one-step" growth curves of MERS-CoV/EMC-2012 and SARS-CoV (Urbani) were established by infecting confluent Calu-3 cells with an MOI of 3, as described above. Cell-free supernatants were harvested at the indicated time points for determining the yields of infectious progeny viruses. (C) Phenotypes of Jurkat T cells transfected with control-versus-CD26/DPP4-encoding plasmid. (D) CD26/DPP4 expression confers the susceptibity of Jurkat T cells to productive MERS-CoV/EMC-2012 infection. (E) Trypan blue exclusion assay was used to simultaneously monitor the viability and mortality of infected Jurkat T cells. **, $P < 0.01$; ***, $P < 0.001$ (Student's *t* test). Data are representative of two independently conducted experiments.

also enable their susceptibility to the infection. Thus, we infected human Jurkat T cells stably transfected with either a human CD26/DPP4-encoded plasmid (Jurkat_CD26DPP4+) or a control plasmid (pcDNA) (Jurkat_C) (15) with MERS-CoV (MOI = 1) and monitored the yields of infectious progeny viruses. As shown in Fig. 1C to E, expression of CD26/DPP4 on Jurkat T cells also readily converted their nonsusceptible state to a susceptible state and then to productive MERS-CoV infection, resulting in ~80% and ~88% cell death within 1 day and 2 days 2 pi, respectively, based on a trypan blue exclusion assay. CD26/DPP4 glycoprotein has been shown to express on many cell types, thereby regulating numerous biological functions, including, but not limited to, activation of T cells and their interaction with antigen-presenting cells (APCs) (16, 17). Provided that subsets of T cells and/or dendritic cells expressing CD26/DPP4 were also as susceptible to MERS-CoV infection, one might anticipate the devastating impact that such an infection could have on the host innate and adaptive immune responses to this newly emerged human respiratory disease.

MERS-CoV has been shown to be more vulnerable than SARS-CoV to prior treatments with IFN-α/λ and IFN-β in primary HAEC and Calu-3 cells, respectively, resulting in either reduced or completely inhibited viral replication (9, 13), suggesting the existence of some variations in the effectiveness of prior IFN treatment of infections by this virus. We compared the relative impact of prior treatment with a high dose of IFN-β (Peprotech) (1,000 U) on the replication of SARS-CoV versus MERS-CoV in Calu-3 cells. We found not only that prior IFN-β treatment for 16 h can significantly reduce the infections of the two viruses (MOI = 0.1) equally well ($P < 0.001$) but also that it can noticeably attenuate the burden of CPE caused by MERS-CoV (Fig. 2), an observation consistent with a recent report (14). Similar to infection with an MOI of 3, MERS-CoV replicates significantly less than does SARS-CoV in Calu-3 cells ($P < 0.05$) when infected at an MOI of 0.1.

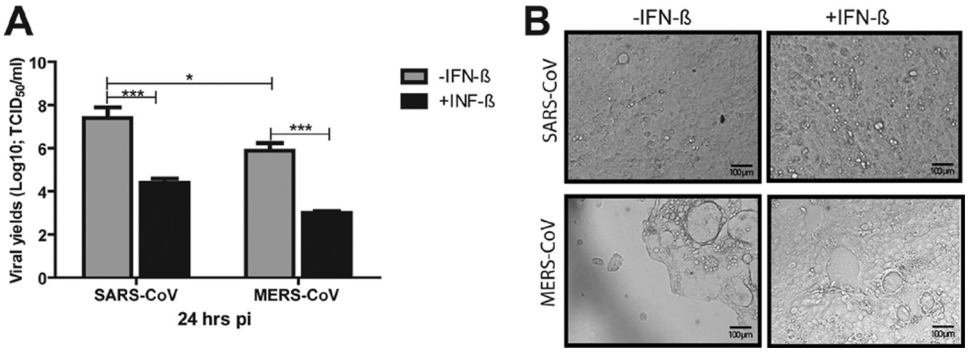

FIG 2 Prior IFN-β treatment effectively inhibits the replication of both SARS-CoV and MERS-CoV and attenuates MERS-CoV-induced CPE. Confluent monolayers of Calu-3 cells, grown in 12-well plates, were treated with recombinant (r) IFN-β for 16 h before being infected with either SARS-CoV or MERS-CoV/EMC-2012 (MOI = 0.1). The resulting cell-free supernatants were harvested at 24 h postinfection (pi) to determine the titers of infectious viruses as described for Fig. 1 (A), whereas the infected monolayer was fixed with paraformaldehyde (4%)–phosphate-buffered saline (PBS) for documentation of MERS-CoV-induced CPE (B). *, $P < 0.05$; ***, $P < 0.001$ (Student's *t* test).

Taken together, our data fail to fully support the earlier notions that MERS-CoV replicates more efficiently in permissive human airway epithelial cells and is more sensitive to IFN-mediated antiviral responses than SARS-CoV (8, 17).

The profound CPE elicited by MERS-CoV-infected Calu-3 cells prompted us to investigate if apoptosis plays any role in this process. We initially analyzed, by confocal microscopy (Olympus FV 1000), Calu-3 cells grown in chamber slides (Nunc Lab-Tek II) infected for 24 h with either SARS-CoV or MERS-CoV (MOI = 0.1), or those remaining uninfected, for the characteristic markers of apoptosis, e.g., unique nuclear morphology and expression of cleaved caspase-3 (CCP3). In contrast to the homogeneously round and smooth nuclei (4′,6-diamidino-2-phenylindole [DAPI] stained) we detected in mock- or SARS-CoV-infected cells (Fig. 3A and B), in MERS-CoV-infected cells, we readily found prominent nuclear margination (arrows, Fig. 3C), chromatin condensation (arrows, Fig. 3C), and typical apoptotic bodies (arrowheads, Fig. 3C) accompanied by CCP3-positive ($CCP3^+$) staining with fluorescein isothiocyanate (FITC)-conjugated anti-CCP3 antibody (Cell Signaling). The latter findings led us to conclude that caspase-dependent apoptosis is likely a prominent mechanism of the aforementioned cell death process. Dual staining with fluorescent annexin V and propidium iodide (PI) in conjunction with flow cytometry-based analyses has been widely used to simultaneously discriminate between and quantify caspase-dependent apoptotic and caspase-independent necrotic cells. Thus, annexin V^+/PI^- staining is regarded as representative of early-stage apoptosis whereas annexin V^+/PI^+ and annexin V^-/PI^+ staining is regarded as representative of late-stage apoptosis or necrosis. Unfortunately, the extreme difficulty in fully dissociating the tightly adherent Calu-3 monolayer into a single-cell suspension, along with the inability to retain PI staining in paraformaldehyde-fixed cells to inactivate residual viruses, a required step for gaining access to our flow cytometry, prohibits us from doing so. Thus, dually FITC-conjugated annexin V- and PI (catalog no. 556570; BD Pharmingen)-stained Calu-3 cells which were infected with MERS-CoV for 12 and 24 h, at MOIs of 0.1 and 3, along with uninfected controls, were subjected to examination by using an inverted phase-contrast fluorescence microscope (Olympus 1X71). In contrast to the essentially negative staining of uninfected (i.e., annexin V^-/PI^-) cells, MERS-CoV-infected cells readily expressed an array of quantitatively different phenotypes, including the most abundant annexin V^+/PI^- staining, followed by annexin V^+/PI^+ staining, and, occasionally, annexin V^-/PI^+ staining, in an infectious dose- and time-dependent manner (Fig. 3D). While dually stained cells were also detected, annexin V^+/PI^- cells emerged as the dominant cell type associated with foci of CPE (Bright field, arrows), emphasizing the critical involvement of apoptosis in MERS-CoV-induced epithelial damage. This notion is best exemplified by cells infected with an MOI of 3, in which the great majority of positively stained cells were either annexin V^+/PI^- (~80%) or annexin V^+/PI^+ (~15%), with very few (if any) annexin V^-/PI^+ at 12 h pi when the infected monolayer remained completely undetached, whereas annexin $V^{-\text{ or weak}}/PI^+$ became the major death phenotype of less than 5% of the monolayer remaining attached at 24 h pi. We also noted that a few clusters of cells retained an annexin V^-/PI^- phenotype (Bright field, arrowheads), which may mean that they survived following the infection for at least 24 h.

The predominant ACE2 expression on the apical surface of Calu-3 cells enables the entry and release of SARS-CoV unilaterally through the apical side (10). We asked whether the entry receptor of MERS-CoV, CD26/DPP4, like ACE2, was also preferentially expressed on the apical domain of Calu-3 cells. To this end, we fixed Calu-3 cells grown onto chamber slides with 4% paraformaldehyde, stained with a primary antibody specifically against human CD26/DPP4 (AF1180; R&D) in combination with an FITC-conjugated secondary antibody (catalog no. A11055; Invitrogen) and assessed their membrane expression of CD26/DPP4 by z-scanning from the bottom, the middle, and the top by using inverted confocal microscopy (Zeiss LSM 710). In contrast to ACE2, which exclusively expresses on the apical domain of Calu-3 cells (10), we noted that CD26/DPP4 indiscriminately expressed on the entire membrane of Calu-3 cells, as revealed by sequential images caught by z-scanning (Fig. 4A), implying that MERS-CoV might be able to infect polarized Calu-3 cells through either the apical or basolateral domains. To test this, we established highly polarized Calu-3 cells in the transwell system (Costar). Briefly, confluent Calu-3 monolayers were allowed to fully differentiate in the presence of an air-liquid interface for an additional 4 days before being subjected to infection with SARS-CoV versus MERS-CoV (MOI = 0.1) via either side of the culture (10). The superna-

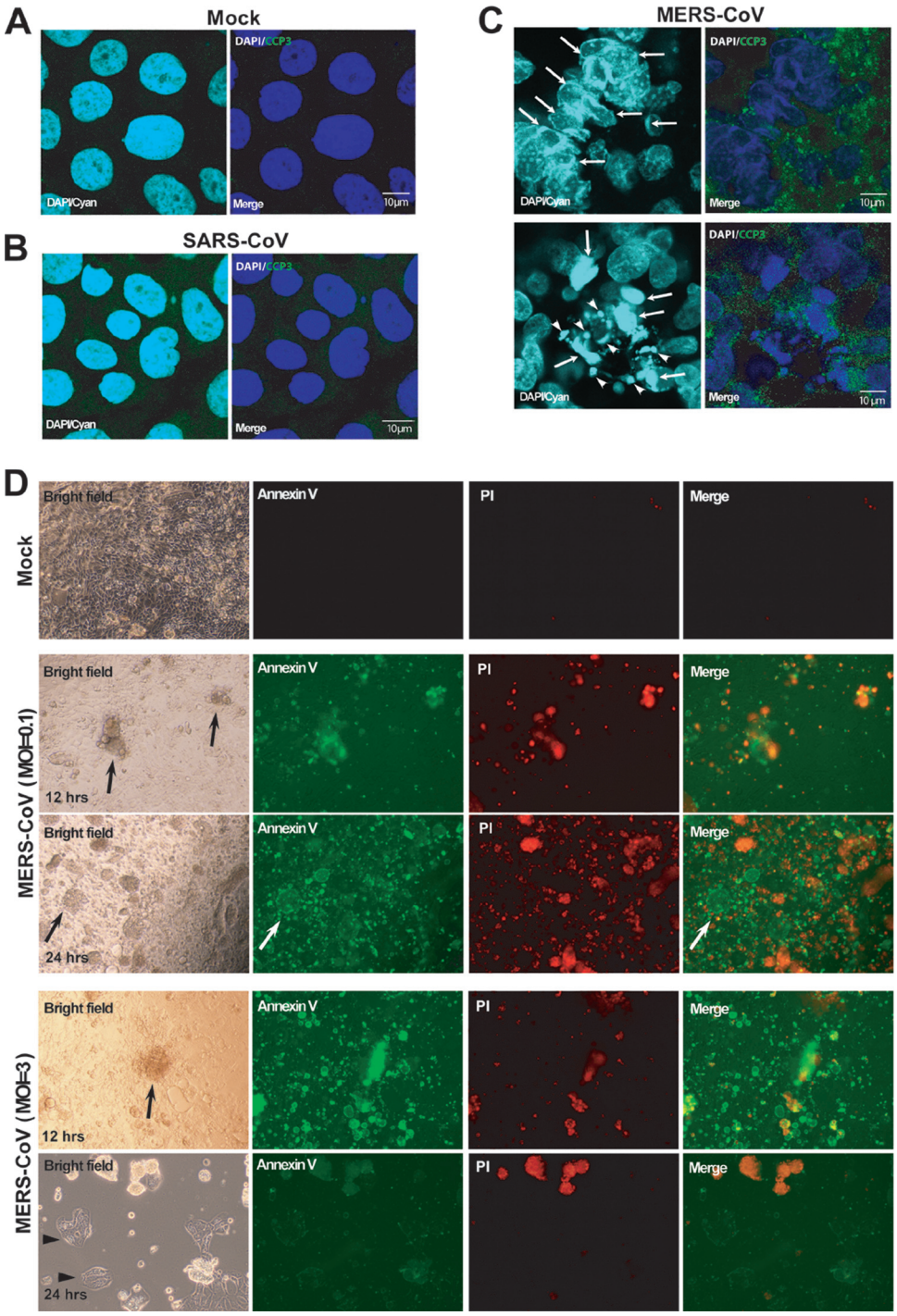

FIG 3 MERS-CoV, but not SARS-CoV, rapidly induces apoptosis of infected Calu-3 cells. Calu-3 cells grown in chamber slides were subjected to either SARS-CoV or MERS-CoV/EMC-2012 (MOI = 0.1) or remained uninfected for 24 h before we analyzed characteristic markers of apoptosis by confocal microscopy. Specifically, the morphology of the nuclei was analyzed after staining with 4′,6-diamidino-2-phenylindole (DAPI), whereas the expression of cleaved caspase 3 (CCP3) was evaluated after staining with Alexa 488-conjugated anti-CCP3 antibodies. The resulting specimens were examined using confocal microscopy at a high magnification. (A and B) Nuclei of mock-infected cells (A) or SARS-CoV-infected cells (B) possess a homogeneously round and smooth morphology without detectable CCP3 expression. (C) In contrast, we readily detected in MERS-CoV/EMC-2012-infected cells prominent nuclear margination, chromatin condensation (arrows), and typical apoptotic bodies (arrowheads) accompanied by positive staining for CCP3 (bright green) in the cytoplasm. (D) Additionally, FITC-conjugated annexin V and propidium iodide (PI) staining was used to discriminate between early apoptotic and late apoptotic/necrotic cells in MERS-CoV/EMC-2012-infected (MOI = 0.1 and 3) and uninfected Calu-3 cultures at both 12 and 24 h pi. Magnification, ×100.

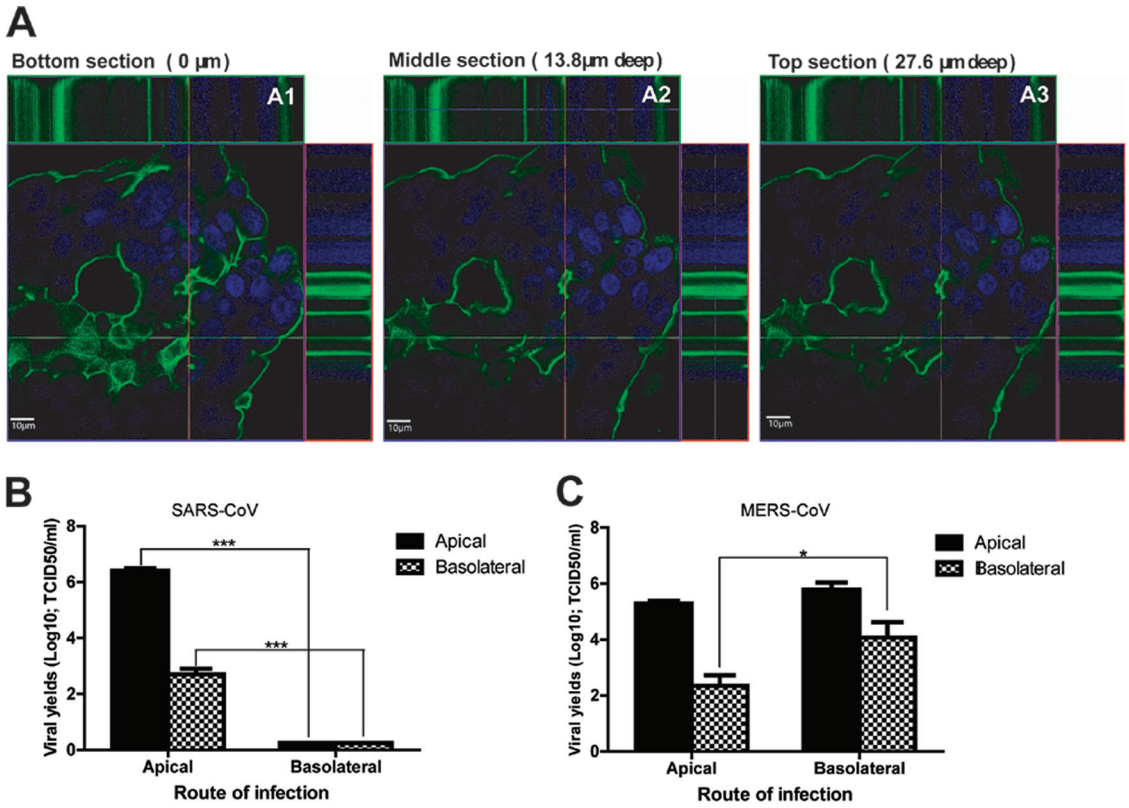

FIG 4 Unbiased apical and basoalteral expression of CD26/DPP4 enables bilateral MERS-CoV entry and release from polarized Calu-3 cells. (A) Confluent Calu-3 cells grown in the chamber slides were subjected to staining for CD26/DPP4 expression. The images of CD26/DPP4 surface expression (green) and nuclear staining (DAPI; blue) were captured by z-stack scanning from the bottom (A1), the middle (A2), and the top (A3) by using an inverted confocal microscope (Zeiss LSM 710). It is clear that CD26/DPP4 is uniformly expressed on the cell membrane of Calu-3 cells. (B and C) Highly polarized Calu-3 cells grown on filter inserts were inoculated with SARS-CoV (B) or MERS-CoV/EMC-2012 (C), at an MOI of 0.1, through either the apical or basolateral surface. At 24 h after infection, the culture supernatants collected from the apical and basolateral chambers were assessed for the contents of infectious viral particles by the $TCID_{50}$ assay. *, $P < 0.05$; ***, $P < 0.001$ (Student's *t* test). The results are derived from representative findings for two independently conducted experiments.

tants harvested at 24 h pi from either chamber were used to determine the yields of progeny viruses. Consistent with our earlier report (10), SARS-CoV infected and released almost exclusively through the apical side of differentiated Calu-3 (Fig. 4B). In contrast, MERS-CoV was indeed capable of doing so through either side of polarized Calu-3 cells (Fig. 4C). While MERS-CoV could be released through both routes, we noted that there was an ~100-fold-higher titer released basolaterally when infection was carried out from the basolateral rather than the apical routes.

Taken together, our results emphasize the fundamental differences in the spread and pathogenesis of these two highly pathogenic human CoVs. Additionally, the ability of MERS-CoV to infect through the basolateral domain of highly differentiated human bronchial epithelial cells is compatible with a blood-borne dissemination of virus, suggesting to us that an additional route other than the respiratory track should be considered for this viral infection.

ACKNOWLEDGMENTS

We thank Heinz Feldmann, National Institutes of Health at Hamilton, MT, and Ron A. Fouchier, Erasmus Medical Center at Rotterdam, The Netherlands, for providing the MERS-CoV/EMC-2012 strain for our study and Mardelle Susman for the editorial assistance. We also thank Leoncio Vergara and Adriana A. Paulucci at Galveston National Laboratory Confocal Microscopy Core and the Optical Microscopy Core (OMC), Center for Biomedical Engineering, Galveston, TX, for their assistance.

This study was supported, in part, by a grant entitled RBD Recombinant Protein-based SARS Vaccine for Biodefense Preparedness (R01AI098775-01-PIs; awarded to P. J. Hotez, M. E. Bottazzi, and S. Jiang) under a subcontract (CON21152) awarded to C.-T.K.T.

REFERENCES

1. **de Groot RJ, Baker SC, Baric RS, Brown CS, Drosten C, Enjuanes L, Fouchier RA, Galiano M, Gorbalenya AE, Memish Z, Perlman S, Poon LL, Snijder EJ, Stephens GM, Woo PC, Zaki AM, Zambon M, Ziebuhr J.** 2013. Middle East respiratory syndrome coronavirus (MERS-CoV); announcement of the Coronavirus Study Group. J. Virol. **87:**7790–7792.
2. **WHO.** 22 May 2013. Novel coronavirus infection—update. WHO, Geneva, Switzerland. http://www.who.int/csr/don/2013_05_22_ncov/en/index.html.
3. **Peiris JS, Guan Y, Yuen KY.** 2004. Severe acute respiratory syndrome. Nat. Med. **10:**S88–S97.
4. **van Boheemen S, de Graaf M, Lauber C, Bestebroer TM, Raj VS, Zaki AM, Osterhaus AD, Haagmans BL, Gorbalenya AE, Snijder EJ, Fouchier RA.** 2012. Genomic characterization of a newly discovered coronavirus associated with acute respiratory distress syndrome in humans. mBio **3:**e00473–12. doi:10.1128/mBio.00473-12.
5. **Mossel EC, Huang C, Narayanan K, Makino S, Tesh RB, Peters CJ.** 2005. Exogenous ACE2 expression allows refractory cell lines to support severe acute respiratory syndrome coronavirus replication. J. Virol. **79:**3846–3850.
6. **Tseng CTK, Huang C, Newman P, Wang N, Narayanan K, Watts DM, Makino S, Packard MM, Zaki SR, Chan TS, Peters CJ.** 2007. Severe acute

respiratory syndrome coronavirus infection of mice transgenic for the human Angiotensin-converting enzyme 2 virus receptor. J. Virol. **81:** 1162–1173.

7. **McCray PB, Jr, Pewe L, Wohlford-Lenane C, Hickey M, Manzel L, Shi L, Netland J, Jia HP, Halabi C, Sigmund CD, Meyerholz DK, Kirby P, Look DC, Perlman S.** 2007. Lethal infection of K18-hACE2 mice infected with severe acute respiratory syndrome coronavirus. J. Virol. **81:**813–821.
8. **Raj VS, Mou H, Smits SL, Dekkers DH, Müller MA, Dijkman R, Muth D, Demmers JA, Zaki A, Fouchier RA, Thiel V, Drosten C, Rottier PJ, Osterhaus AD, Bosch BJ, Haagmans BL.** 2013. Dipeptidyl peptidase 4 is a functional receptor for the emerging human coronavirus-EMC. Nature **495:**251–254.
9. **Kindler E, Jonsdottir HR, Muth D, Hamming OJ, Hartmann R, Rodriguez R, Geffers R, Fouchier RA, Drosten C, Muller MA, Dijkman R, Thiel V.** 2013. Efficient replication of the novel human betacoronavirus EMC on primary human epithelium highlights its zoonotic potential. mBio **4:**e00611–12. doi:10.1128/mBio.00611-12.
10. **Tseng CTK, Tseng J, Perrone L, Worthy M, Popov V, Peters CJ.** 2005. Apical entry and release of severe acute respiratory syndrome-associated coronavirus in polarized Calu-3 lung epithelial cells. J. Virol. **79:**9470–9479.
11. **Chan PK, To KF, Lo AW, Cheung JL, Chu I, Au FW, Tong JH, Tam JS, Sung JJ, Ng HK.** 2004. Persistent infection of SARS coronavirus in colonic cells in vitro. J. Med. Virol. **74:**1–7.
12. **Müller MA, Raj VS, Muth D, Meyer B, Kallies S, Smits SL, Wollny R, Bestebroer TM, Specht S, Suliman T, Zimmermann K, Binger T, Eckerle I, Tschapka M, Zaki AM, Osterhaus AD, Fouchier RA, Haagmans BL, Drosten C.** 2012. Human coronavirus EMC does not require the SARS-coronavirus receptor and maintains broad replicative capability in mammalian cell lines. mBio **3:**e00515–12. doi:10.1128/mBio.00515-12.
13. **Zielecki F, Weber M, Eickmann M, Spiegelberg L, Zaki AM, Matrosovich M, Becker S, Weber F.** 2013. Human cell tropism and innate immune system interactions of human respiratory coronavirus EMC compared to those of severe acute respiratory syndrome coronavirus. J. Virol. **87:**5300–5304.
14. **de Wilde AH, Ray VS, Oudshoorn D, Bestebroer TM, van Nieuwkoop S, Limpens RW, Posthuma CC, van der MY, Barcena M, Haagmans BL, Snijder EJ, van den Hoogen BG.** Human coronavirus-EMC replication induces severe in vitro cytopathology and is strongly inhibited by cyclosporine or interferon-alpha treatment. J. Gen. Virol. doi:10.1099/vir.0.052910-0, in press.
15. **Morimoto C, Lord CI, Zhang C, Duke-Cohan JS, Letvin NL, Schlossman SF.** 1994. Role of CD26/dipeptidyl peptidase IV in human immunodeficiency virus type 1 infection and apoptosis. Proc. Natl. Acad. Sci. U. S. A. **91:**9960–9964.
16. **Ohnuma K, Yamochi T, Uchiyama M, Nishibashi K, Yoshikawa N, Shimizu N, Iwata S, Tanaka H, Dang NH, Morimoto C.** 2004. CD26 up-regulates expression of CD86 on antigen-presenting cells by means of caveolin-1. Proc. Natl. Acad. Sci. U. S. A. **101:**14186–14191.
17. **Ikushima H, Munakata Y, Ishii T, Iwata S, Terashima M, Tanaka H, Schlossman SF, Morimoto C.** 2000. Internalization of CD26 by mannose 6-phosphate/insulin-like growth factor II receptor contributes to T cell activation. Proc. Natl. Acad. Sci. U. S. A. **97:**8439–8444.
18. **Fuk-Woo Chan J, Chan KH, Choi GKY, To KKW, Tse H, Cai JP, Yeung ML, Cheng VCC, Chen H, Che XY, Lau SKP, Woo PCY, Yuen KY.** 2013. Differential cell line susceptibility to the emerging novel human betacoronavirus 2c EMC/2012: implications for disease pathogenesis and clinical manifestation. J. Infect. Dis. **207:**1743–1752.
19. **Josset L, Menachery VD, Gralinski LE, Agnihothram S, Sova P, Carter VS, Yount BL, Graham RL, Baric RS, Katze MG.** 2013. Cell host response to infection with novel human coronavirus EMC predicts potential antivirals and important differences with SARS coronavirus. mBio **4:**e00165–13. doi:10.1128/mBio.00165-13.